International Journal of Technology 15(3) 628-640 (2024)
Received October 2021 / Revised December 2021 / Accepted March 2022

International Journal of Technology

Analysis of Combined Braking Torque on The Regenerative Anti-Lock Braking System in The Quarter Electric Vehicle Model

Katherin Indriawati[1*], Bambang Sudarmanta[2], Bambang Lelono Widjiantoro[1], Nur Adlun Hafiizh[1], Ahmad Hazmi Said[1]

[1]*Department of Engineering Physics, Institut Teknologi Sepuluh Nopember, Kampus ITS Sukolilo–Surabaya, 60111, Indonesia*
[2]*Department of Mechanical Engineering, Institut Teknologi Sepuluh Nopember, Kampus ITS Sukolilo–Surabaya, 60111, Indonesia*

Abstract. The regenerative ABS is developed to avoid slip and to regenerate energy using two types of braking: friction and motor. This paper discusses the experimental results of combining the two types of braking which are applied to a quarter-electric vehicle model. The control algorithm is developed using sliding mode control (SMC), where continuous action is performed to produce motor braking torque while discrete action is performed to produce hydraulic braking torque (friction). Furthermore, the proposed control system also implements control coordination to distribute braking torque, enhances the occurrence of the non-slip process, and generates energy for vehicle batteries. From the experimental results, it is concluded that the slip ratio value can be used to obtain the optimum conditions for the braking process, where the hydraulic torque as the cause of the slip, is limited through the braking distribution algorithm. The proposed control system produces a response with a brake speed of 2 m/s and a 3.39% increase in battery SOC.

Keywords: Anti-lock braking system; Control coordination; Regenerative; Sliding mode control

1. Introduction

One of the efforts to reduce the negative impact of fossil fuel vehicles is the development and use of electric vehicles. Generally, when braking occurs, energy is wasted in the form of heat due to friction between the brake pads and the wheels. Energy wastage is an important issue, especially for electric vehicles. Therefore, this led to the design of a regenerative braking system capable of converting kinetic energy into electricity when vehicles decelerate. This energy is then stored in batteries for reuse, thereby increasing vehicle efficiency (Usman *et al.*, 2016; Benetti *et al.*, 2014; Faria and Delgado, 2014). The braking torque is generated by the motor driving the vehicle. The results showed that the energy storage achieved by this system is in the range of 8%-25% of the total energy used by the vehicle, which is dependent on the regulatory cycle and control strategy, in addition to manipulation of braking components such as the use of electric brake boosters which can reduce electricity consumption (Nugraha *et al.*, 2021; Shah *et al.*, 2018; Yu, Liu and Liu, 2016). Conversely, the braking torque of the motor is often not capable of braking quickly, due to many influencing factors, such as motor speed, charging status, and battery

*Corresponding author's email: katherin@ep.its.ac.id, Tel.: +62-31-5947188
doi: 10.14716/ijtech.v15i3.5265

temperature (Rajendran *et al.*, 2018; Li, Du, and Li, 2016; Tehrani *et al.*, 2011; Zhang, Yin, and Zhang, 2010). Therefore, the process of braking with hydraulic torque is still needed.

Generally, the braking system plays an essential role in the safety of vehicles. The latest technology commonly used to prevent the wheels of vehicles from being locked during the sudden application of brakes is the anti-lock braking system (ABS). According to preliminary studies, sudden braking leads to directional instability such as understeer or oversteer. Braking force is influenced by several factors, such as road and tire conditions, coefficient of friction, etc. Unlike the conventional braking system, in the ABS, the wheels are kept from being locked with a certain slip state where the coefficient of adhesion between the road and the tires is the greatest. This makes the braking distance shorter, and the vehicle remains stable or easy to control. Therefore, cars with ABS have the ability to reduce the stopping distance and increase maneuverability compared to those without this system (Fernandez *et al.*, 2021; Aksjonov, Augsburg, and Vodovozov, 2016; Aly *et al.*, 2011).

This process significantly increases a vehicle's safety in extreme conditions due to its ability to maximize tire-road friction while maintaining a large lateral (directional) force that ensures its control (Reif, 2014; Oleksowicz *et al.*, 2013; Sergio and Mara, 2010). According to Kim and Lee (2013), an optimum slip ratio value maximizes the coefficient of friction in all road conditions. Therefore, a suitable control strategy is to maintain the slip ratio value to ensure the braking system's optimal and safe working range.

Designing an anti-lock braking system is a fairly complicated design process. Here, one of the main obstacles is in determining the nonlinearity and uncertainty. Some advanced control approaches have been proposed for ABS, such as fuzzy (Berouaken and Boulahia, 2015; Yazicioglu and Unlusoy, 2008; Mirzaei *et al.*, 2005), fuzzy-neural (Lin and Le, 2017; Wang, Chen, and Su, 2012; Chen *at al.*, 2006), sliding mode (Guo, Jian, and Lin, 2014; Guo and Wang, 2012), model predictive control (He *et al.*, 2021; Yuan *et al.*, 2015), and other intelligent controls (Mirzaeinejad, 2018; Boopathi and Abudhahir, 2016; Topalov *et al.*, 2011).

The use of regenerative braking as ABS was proposed by Tur, Ustun, and Tuncay (2007). Simulation comparisons between ABS with motor and hydraulic braking torques were also carried out in this research. Next, the analysis of the combination of the regenerative braking system and ABS is carried out (Bera, Bhattacharyya, and Samantaray, 2011) using the sliding mode controller approach. This combination is one of the innovative technological processes to improve vehicle performance. The combined braking also serves to avoid overvoltage problems in electric vehicles as discussed in Yusivar *et al.* (2015). However, research on the combination of the two braking torques is still small especially when it comes to ABS.

This paper discusses the combination of hydraulic torque and motor torque in the ABS system to form a braking system called regenerative ABS. In this case, the effect of both types of braking torque on the ABS regenerative system is analyzed based on experimental data on the prototype of a quarter-electric vehicle model. For this purpose, the prototype regenerative ABS is designed, with the controller installed in the motor and the hydraulic brakes. The built system is also equipped with a braking distribution mechanism to coordinate the working mechanism of both braking torques. SMC approach is used as a control algorithm, and its performance is compared with gain-scheduling PID.

2. Regenerative ABS Plant

The Regenerative Anti-lock Braking System (ABS) Plant in this research is applied to a single-wheel electric vehicle model, which only uses one-wheel representation. The top represents the wheel speed connected to a hydraulic braking system. Meanwhile, the

bottom denotes the vehicle's speed and is connected to a Brushless Direct Current (BLDC) motor driver. The scheme of the regenerative ABS plant carried out in this research is shown in Figure 1.

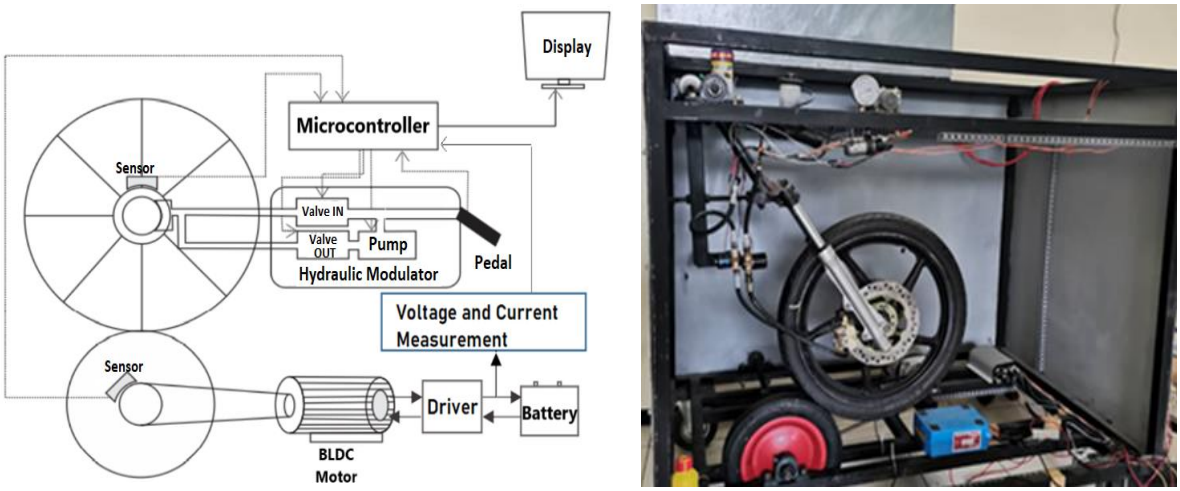

(a) (b)

Figure 1 Schematic of the regenerative ABS plant (a) and the setup of the plant (b)

This plant consists of a battery that functions as a voltage source used by a motor driver to turn on and regulate the vehicle. Therefore, electrical braking occurs when the driver regulates the stator current, thereby producing attractive and repulsive forces on the BLDC. Furthermore, this process is used to drive the bottom and top wheels, usually zero at the point of contact. Generally, the braking system with hydraulic torque occurs in vehicles by stopping the top wheels using brake calipers, which decreases speed until they stop turning. In this case, a hydraulic modulator is used to regulate the duration of braking. When a driver applies the brake to a vehicle, the microcontroller receives speed data and reacts to the braking module. The control algorithm used is a sliding mode control (SMC) approach. The top and bottom wheel speed response graphs are shown on the monitor screen.

The hydraulic modulator consists of two on-off solenoid valves and one pump. The solenoid valve works in reverse condition, depending on which operating position is needed as described in Budiono *et al.* (2020). However, during non-braking conditions, the input valve is closed while the output is opened. This means that the system becomes dumped, thereby trapping the brake fluid. Conversely, when braking is required, the output valve closes, and the input valve opens enabling the flow of brake fluid into the calipers and stopping the wheels. The pump is used to replace the function of the brake pedal in every operating condition.

When brakes are applied, the BLDC changes its function from a motor to a generator. The specifications of the motor used in this research are shown in Table 1. This regenerative process reverses the current in the motor-battery circuit during deceleration and directs it to the battery. This condition is measured by the estimated state of charge (SOC) value. Therefore, it is necessary to measure V_{use}, the value of the battery voltage when in use, using the equation (1):

$$SOC\ (\%) = \frac{V_{use}}{V_{full}} \times 100\% \qquad (1)$$

where V_{full} is the voltage when the battery is full.

Table 1 Motor Specification

Item	Value
Model	BM1418ZXF
Rated Output Power	750 W
Rated Voltage	48/60V DC
Speed after Reduction	480RPM
Rated Speed	2800RPM
Full Load Current	≤ 20.0/16.0 A
No Load Current	≤ 5.0/4.5 A
Rated Torque/Full Torque	2.56 N.m / 14.92 N.m
Efficiency	≥ 75 %
Gear Ratio	1:6

The slip ratio value is calculated using the equation (2):

$$\lambda = \frac{v - r_{\omega}\omega_{\omega}}{v} \quad (2)$$

where
v is the lateral (vehicle) speed of the bottom wheel
ω_{ω} is the angular speed of the top wheel
r_{ω} is the top wheel radius at 0.275 m

The measurement module components at this plant include a speed sensor that measures wheel and vehicle speed, a current sensor used to determine the reverse current during regenerative braking, and a voltage divider circuit for the battery voltage.

The speed sensor in this system uses proximity, generating two signal conditions of high and low. The signal is high when the sensor touches the ring, and low assuming it does not detect the ring. Furthermore, the sensor outputs a value when the ring rotates once. However, a signal conditioning circuit needs its rotation value to reach a revolution per minute (rpm) before entering the microcontroller. The proximity sensor works to read the angular speed value ω (rpm) on the top and bottom wheels (vehicle representation). At the bottom, the angular speed value is converted to the lateral v (km/h) with the equation (3):

$$v = 0{,}06\ \pi D\ \omega \quad (3)$$

where D is the diameter of the bottom wheel at 0.32 m.

A voltage divider circuit is used on the battery-microcontroller line to measure the battery voltage. This is necessary because the total voltage on the battery is around 50 Volts, while the microcontroller's analog input pin is only capable of reading a maximum of 5 Volts. The voltage divider circuit used in this plant uses 2 resistors of 10K and 100K Ohms at 5% tolerance, respectively.

Current measurement is carried out using an integrated circuit (IC) which detects AC and DC. This sensor works according to the Hall Effect theory, where a conductor is positioned close to the IC to create a magnetic field, converted into a proportional voltage. This analog voltage is read by the microcontroller and converted to a current value in amperes.

3. Regenerative ABS Control System

3.1. Sliding Mode Control Approach

This research created a closed-loop system for a regenerative ABS plant (Figure 2) using a sliding mode control (SMC) suitable for plants with high nonlinearity characteristics such as ABS. In this case, the controlled variable is the slip ratio λ, which can be calculated

using the measured speed value of the vehicle (V_{meas}) or the wheel (w_{meas}). Therefore, it has the ability to overcome the locked wheels when braking. The control system is expected to set the slip ratio response around the setpoint value $\lambda_{setpoint}$ of 0.2, which is the optimum value for dry and straight asphalt road conditions (Guo and Wang, 2012).

The control signal with the SMC algorithm is generated using the nonlinear equation (4):

$$u = K_p s + \frac{1}{B} K\ sign(s) \tag{4}$$

where:

$$B = \frac{1}{v} \frac{r_\omega}{J_\omega}$$

J_ω is the inertia moment of the wheel at 1 Nm
K_p is the proportional gain
K is controller gain
s = sliding surface = setpoint error (slip ratio error)

The signum (sign) function is defined using (5):

$$sign(s) = \begin{cases} 1\ , s > 0 \\ -1\ , s < 0 \end{cases} \tag{5}$$

The SMC result is a control signal that represents the required braking torque, T_{breq}. The motor braking torque in this research is carried out in full power from start to finish using a PWM signal with a duty cycle of 100%. Therefore, continuous and discrete braking actions are performed to produce motor and hydraulic (friction) braking torques.

The required motor braking torque T_{mreq} is computed using a linear function of sliding surface as (6):

$$T_{mreq} = K_p s \tag{6}$$

Meanwhile, the hydraulic braking torque required T_{hreq} is the second-term part of (4), namely (7):

$$T_{hreq} = \frac{1}{B} K\ sign(s) \tag{7}$$

The controller gain values K_p and K from the SMC algorithm are determined by trial and error.

The control system adjusts the solenoid valve, which functions as an actuator to the control signal (volt). In its application, the hydraulic braking torque control signal is represented in the form of a delay. The ABS valve is controlled by 2 types of solenoids, which open and close the diaphragm to provide and relieve pressure on the brake chamber. As stated earlier, the first solenoid opens when braking and closes when the reverse is the case. Meanwhile, the second solenoid closes when braking and vice versa. Therefore, the required hydraulic braking torque is embodied in the form of braking duration or the microcontroller language using the term delay, namely (8):

$$t_{delay} = \frac{T_{hreq}}{T_{hmax}} T_s \tag{8}$$

where T_{hmax} is the hydraulic torque at maximum speed and T_s is the sampling time.

The controller uses switching operations on the inverter. During the braking process, the inverter is tasked with increasing the back electromotive force (BEMF) voltage for current to flow into the battery. The braking energy is then stored in the battery, while the proportional control method is used to control the PWM signal on the inverter. Furthermore, the proposed system is very simple and efficient because it uses a switching

operation on the inverter hence it does not require additional electronic components to perform regenerative braking.

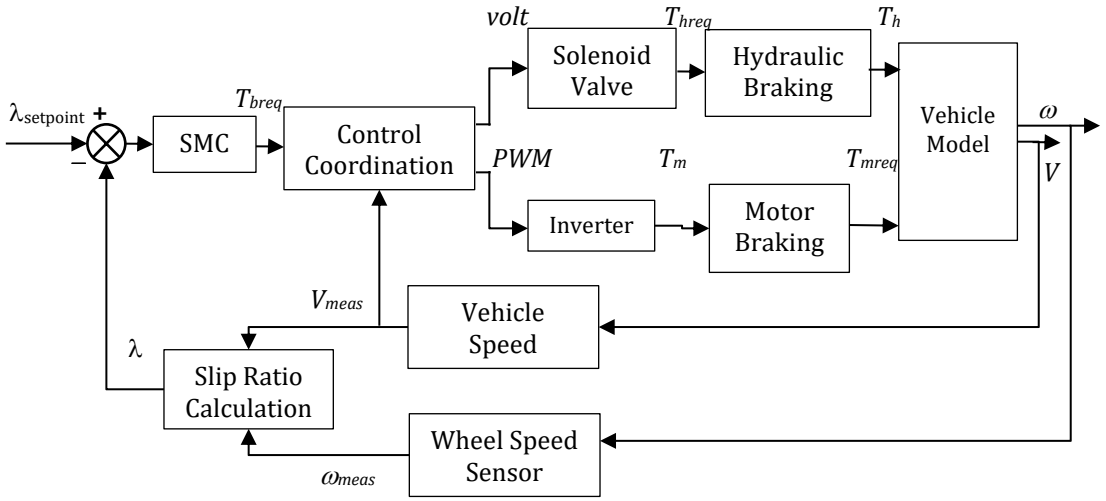

Figure 2 Block diagram of the slip ratio control system with SMC

3.2. Control Coordination

In an effort to obtain regenerative energy in the motor braking section, it is necessary to regulate the braking torque distribution. This distribution algorithm is expected to make braking time faster with significant regenerative energy. In this research, the distribution of braking (control coordination) is designed based on the threshold value of the slip ratio, λ_{thr}. When it is smaller than λ_{thr}, the braking torque that works is hydraulic and motor. However, when the slip ratio is greater than λ_{thr}, only the motor works. The braking distribution then allows the torque to run from start to finish but regulates the stopping time of the hydraulic because it causes locked wheels. Furthermore, a controller is needed for the proper functioning of the hydraulic braking torque to prevent slippage. In this case, the controller algorithm used is SMC and the control coordination is able to stop the vehicle quickly and without slipping. The braking distribution algorithm is shown in Figure 3. λ_{thr} is selected based on the open-loop test results of combined regenerative braking (motor and hydraulic torque). The largest slip ratio value that occurs just before the slip is used to determine the λ_{thr} value. When electro-hydraulic braking is used, here the electric braking torque is made to work at its maximum (PWM duty cycle is 100%), and the lack of braking torque is overcome by hydraulic braking torque. So for high speed, braking can still be done. A more detailed explanation is given in section 4 of this paper.

The regenerative performance of the ABS control system is evaluated by the SOC value and the integral of the time-multiplied absolute value of error (ITAE) which quantitatively characterizes the deviation from the actual wheel slip ratio value from the setpoint. Other performances include braking distance, brake speed, and average deceleration.

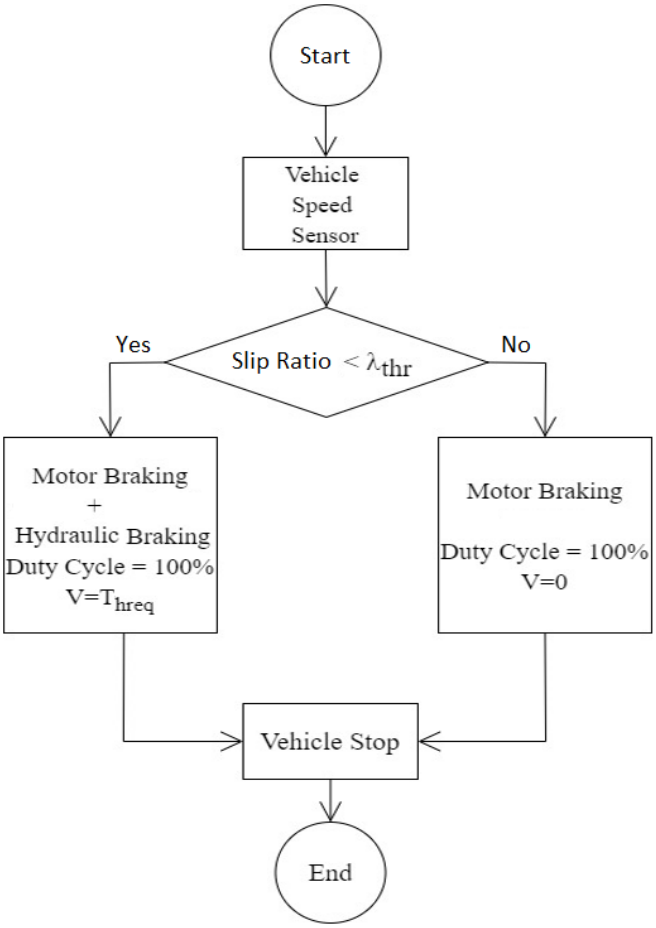

Figure 3 The proposed braking distribution algorithm

4. Results and Discussion

4.1. Analysis of the Effect of Braking Torque

A plant test is carried out until the car stops in an open loop or without involving a controller. There were 3 braking experiments, namely electric, hydraulic, and electric-hydraulic.

The open-loop test response results for electric and hydraulic braking experiments are shown in Figures 4(a) and 4(b), i.e. slip ratio value and speed, respectively. The result indicates that hydraulic braking with constant torque (5.5 Nm) produces a more significant effect than the motor, as shown in Figure 5(a). Therefore, at 0.6 seconds, the system with hydraulic braking only locks the wheels (zero speed) with a slip ratio value of 1 and the vehicle stops at 1.2 seconds. Meanwhile, motor braking causes the vehicle to stop at 1.6 seconds without slip events because the ratio is around ±0.2.

The regenerative energy generated from the motor braking experiment increases the SOC value, as shown in Figure 5(b). At the beginning of the braking process, the SOC value, originally at 86.4%, increases until the wheel stops at 90.3%. Therefore, the SOC value of the battery is increased by 3.9%.

Based on this experiment, it can be concluded that the slip event occurs due to the hydraulic braking torque, which needs to be adjusted without causing the wheels to lock.

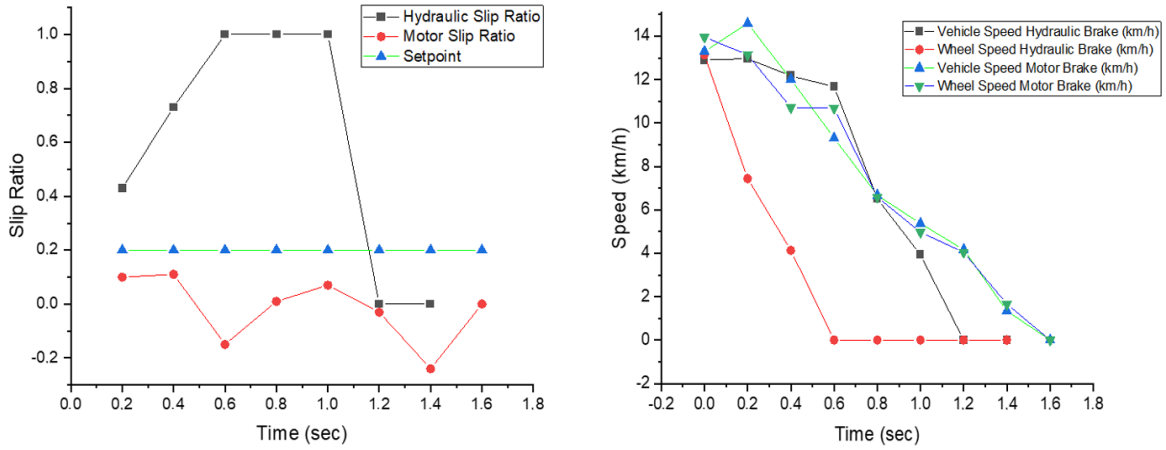

(a) (b)

Figure 4 Slip ratio response (a) and speed response (b) during open-loop plant test with hydraulic or motor braking

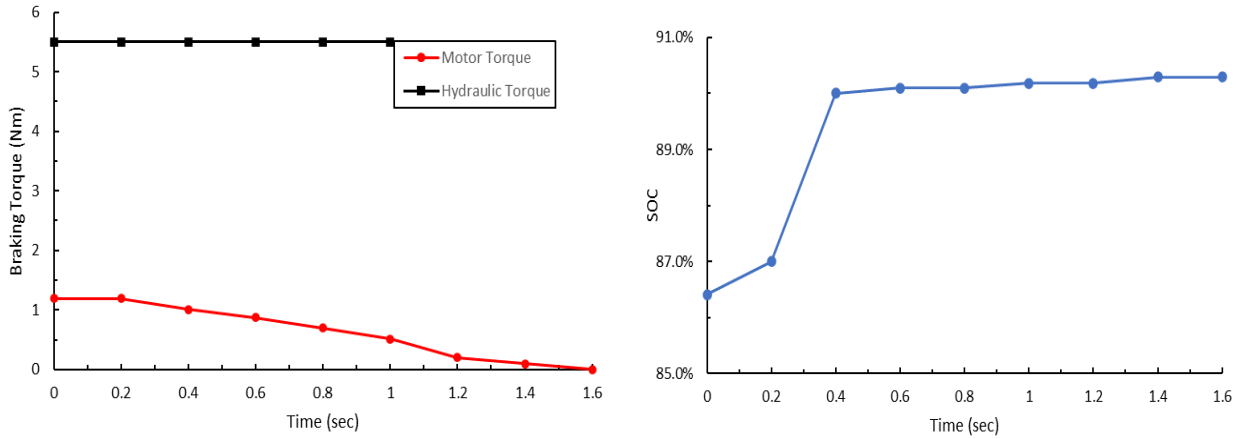

(a) (b)

Figure 5 Braking torque during individual tests (a) and SOC increase in the case of motor braking torque (b)

The open-loop test response results for the electric-hydraulic combined braking experiment are shown in Figures 6(a) for slip ratio value and (b) for speed. The combined braking torque causes the wheels to lock at 0.6 seconds, which is similar to the application of hydraulic braking torque. However, the combined process causes the braking time to be faster. In conclusion, the addition of motor braking torque accelerates the braking time without changing the slip condition. Furthermore, the motor braking needs to be carried out with the maximum motor braking torque to make the maximum possible regenerative energy. Therefore, a braking distribution algorithm is needed to regulate the regenerative energy storage without causing slippage.

The threshold value for distributing braking λ_{thr} is determined based on the results of the slip ratio response in Figure 6(a). Its value of 0.58 is obtained at 0.4 seconds just before the wheels are locked. Therefore, the slip ratio threshold must be below this value. The braking distribution algorithm applied in this research uses the λ_{thr} = 0.4.

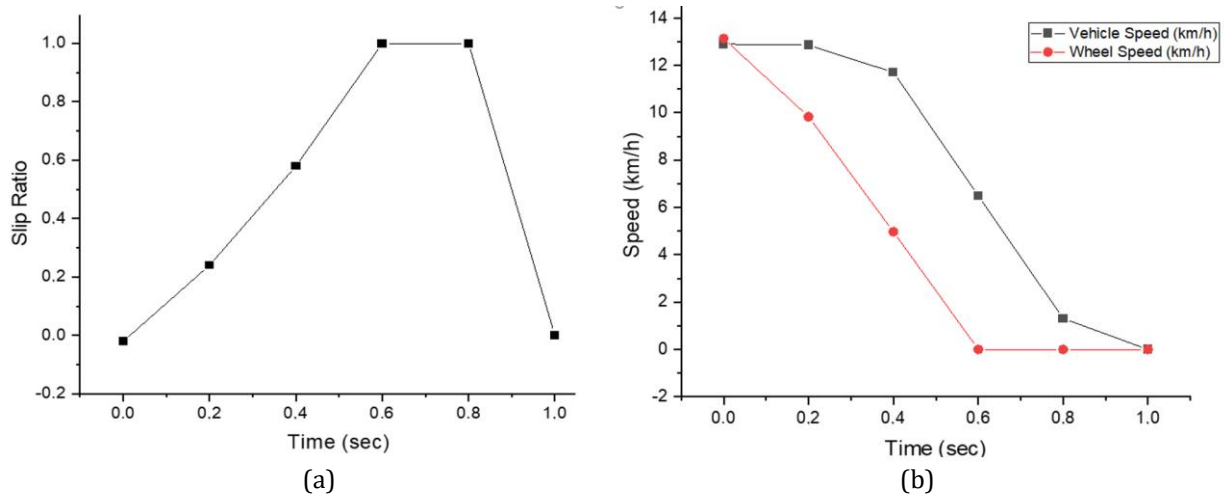

(a) (b)

Figure 6 Slip ratio (a) and speed response (b) during the open-loop plant test

4.2. Control System Response Result

The required motor torque value in Equation (6) is proportional to the setpoint error deviation value, with a controller gain K_p of 13. However, this value cannot be fulfilled entirely due to several factors influencing the motor torque. In this case, the motor braking torque is proportional to the motor speed and the hydraulic braking torque is equal to the required value, which is calculated by equation (7). Based on the experimental results, it is found that the best controller K gain value is 0.001.

The braking distribution algorithm works based on the slip ratio value, which uses the value of λ_{thr} = 0.4 as described in the previous section. The braking distribution graph shown in Figure 7 indicates that the hydraulic braking torque is no longer constant and reduces with a decrease in speed. The vehicle stops at 1.2 seconds (Figure 8(a)). At the time of 1 second, only the braking torque of the motor works because the slip ratio in the 0.8 seconds has already passed λ_{thr}, as shown in Figure 8(b). In total, the braking torque initially reached 7 N.m, however, it decreased until at 0.6 seconds to reach 3.1 N.m, therefore causing the wheels to unlock as in the case of braking with constant hydraulic torque (without controller). In this case, no more slip events occur, and the ratio value is maintained around 0.2 as shown in Figure 8(b).

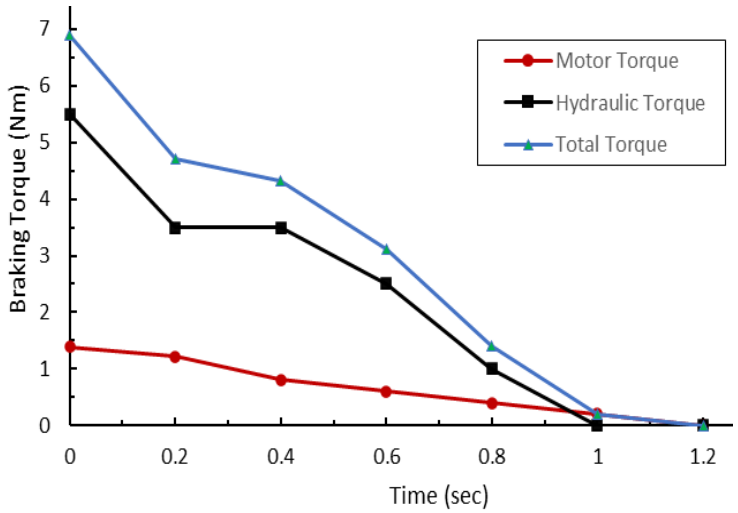

Figure 7 Distribution of braking torque of the regenerative ABS control system

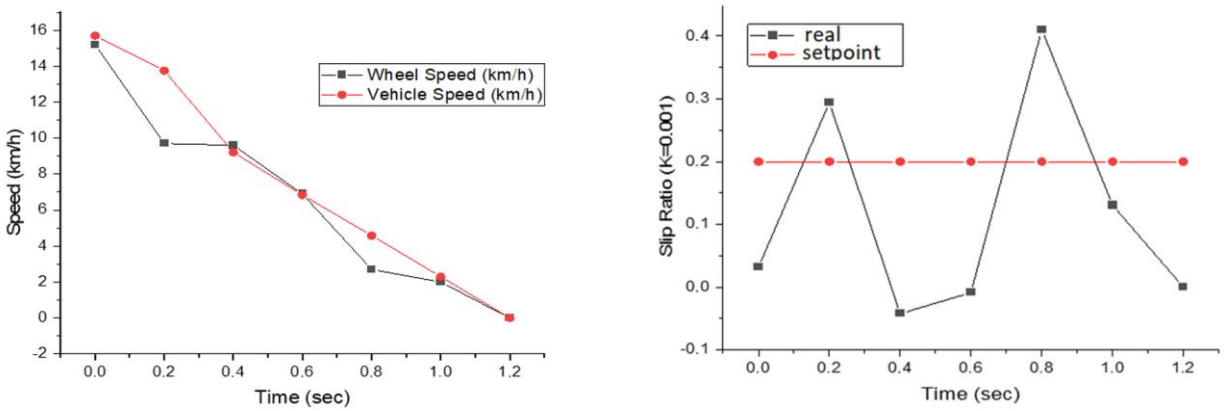

(a) (b)

Figure 8 Speed response (a) and slip ratio response (b) of the regenerative ABS control system

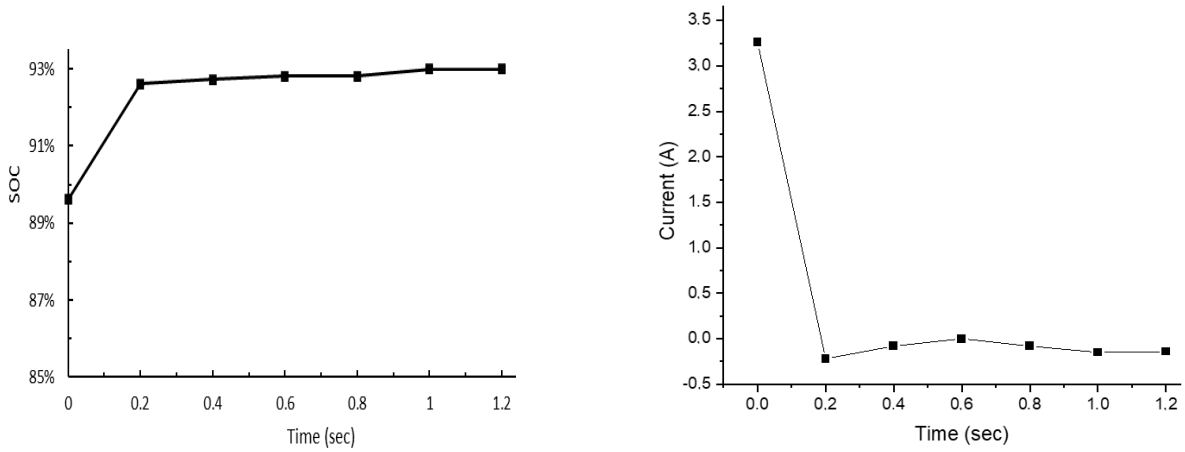

(a) (b)

Figure 9 SOC value (a) and current value (b) of regenerative ABS control system

Figure 9(a) shows the changes in SOC values due to regenerative energy conversion. Overall, there was a 3.4% increase in SOC from 89.61% to 93%. Therefore, the regenerative energy generated from the regenerative ABS control system is smaller than in the case of motor braking alone at 4.7%, as shown in Figure 5(b). This is due to the distribution of braking torque between the motor and hydraulic torque, hence the brake speed is increased without causing the slip.

Figure 9(b) shows the response of the motor current during braking at 3.26 A. Furthermore, when the motor brakes, the current value changes to -0.08 A, thereby indicating that the current direction is no longer to the motor but to the battery. This indicates the conversion of mechanical energy with a torque value of 1.38 N.m into the electrical current of 3.34 A, at the beginning of the braking process. The regenerative energy generated is then significantly reduced as the speed decreases, with a current below 0.25 A.

The regenerative ABS control system is expected to make non-slip braking run quickly with the maximum possible generation of regenerative energy. When the λ_{thr} value used is less than 0.4, the braking time becomes longer, and the regenerative energy is greater. Meanwhile, when the λ_{thr} value is greater, the braking time becomes faster with smaller regenerative energy. Therefore, it can be concluded that there is a trade-off between

braking speed and energy recovered. This led to the process of optimizing problems associated with the λ_{thr} variable, which is interesting to be used as a topic for further research.

The ABS regenerative control system using the SMC approach is compared to its performance with the proportional gain scheduling approach which is also conducted in this research. The results of the performance comparison are shown in Table 2. It shows that the SMC approach is slightly superior in all aspects, including ITAE. Thus, it can be concluded that the type of nonlinear control algorithm is not the main determinant for the performance of the combined braking system, but it is the coordination control that determines the performance of the regenerative ABS.

Table 2 Comparison of Control Scheme Performance

No	Scheme	Average Deceleration (m/s^2)	Braking Distance (m)	ITAE	SOC (%)	Brake Speed (m/s)
1	SMC	0.726	2.473	0.719	3.39 %	2.025
2	Proportional Gain Scheduling	0.63	2.38	0.71	2.43 %	1.983

5. Conclusions

In conclusion, the regenerative ABS control system equipped with a braking distribution feature has the ability to produce fast non-slip braking action and increase the battery SOC by almost 4%. The continuous action of the motor braking torque plays a role in accelerating the braking time in addition to generating regenerative energy. Meanwhile, the discrete action of hydraulic braking torque plays a role in accelerating braking time and needs to be limited to avoid slipping through coordinated control based on the threshold value of the slip ratio. Therefore, the process of determining this threshold value can be used as a topic for future research to achieve optimum regenerative braking conditions.

Acknowledgments

The authors are grateful to the Institut Teknologi Sepuluh Nopember for their financial support under the Collaboration Research Centre project scheme (reference 1159/PKS/ITS/2021).

References

Aly, A.A., Zeidan, E.S., Hamed, A., Salem, F., 2011. An Antilock-Braking Systems (ABS) Control: A Technical Review. *Intelligent control and Automation*. Volume 2(03), pp. 186

Aksjonov, A., Augsburg, K., Vodovozov, V., 2016. Design and Simulation of The Robust ABS and ESP Fuzzy Logic Controller on The Complex Braking Maneuvers. *Applied Sciences*, Volume 6(12), p. 382

Bera, T.K., Bhattacharyya, K., Samantaray, A.K., 2011. Bond Graph Model-Based Evaluation of a Sliding Mode Controller for Combined Regenerative and Antilock Braking System. *Part I Journal System Control Engineering,* Volume 225, pp. 918–934

Benetti, G., Delfanti, M., Facchinetti, T., Falabretti, D., Merlo, M., 2014. Real-Time Modeling and Control of Electric Vehicles Charging Processes. *IEEE Transactions on Smart Grid*, 6(3), pp. 1375–1385

Berouaken, A., Boulahia, R., 2015. Fuzzy Control of Anti-Lock Braking System And Active Suspension In A Vehicle. *Sciences & Technologie*. B, Sciences de l'ingénieur, Volume 2015, pp. 41–45

Boopathi, A.M., Abudhahir, A., 2016. Adaptive Fuzzy Sliding Mode Controller for Wheel Slip Control in Antilock Braking System. *Journal of Engineering Research*, Volume 4, pp. 1–19

Budiono, H.D.S., Sumarsono, D.A., Adhitya, M., Baskoro, A.S., Saragih, A.S., Prasetya, S., Zainuri, F., Nazaruddin, Heryana, G., Siregar, R., 2020. Development of Smart Magnetic Braking Actuator Control for A Heavy Electric Vehicle. *International Journal of Technology*, Volume 11(7), pp. 1337–1347

Chen, G.M., Wang, W.Y., Lee, T.T., Tao, C.W., 2006. Observer-Based Direct Adaptive Fuzzy-Neural Control for Anti-lock Braking Systems. *International Journal of Fuzzy Systems*, 8(4).

Faria, M., Delgado, 2014. Managing The Charging of Electrical Vehicle: Impacts on The Electrical Grid and on The Environmental. *Intelligent Transportation Systems Magazine IEEE,* Volume 6(3), pp. 54–65

Fernández, J.P., Vargas, M.A., García, J.M.V., Carrillo, J.A.C., Aguilar, J.J.C., 2021. Coevolutionary Optimization of A Fuzzy Logic Controller For Antilock Braking Systems Under Changing Road Conditions. *IEEE Transactions on Vehicular Technology*, Volume 70(2), pp. 1255–1268

Guo, J., Jian, X., Lin, G., 2014. Performance Evaluation of an Anti-Lock Braking System for Electric Vehicles with a Fuzzy Sliding Mode Controller. *Energies,* Volume 7(10), pp. 6459–6476

Guo, J., Wang, J., 2012. Application of Sliding Mode Control for Electric Vehicle Antilock Braking Systems. *Advanced Materials Research,* Volume 505*,* pp. 440–446

He, Z., Shi, Q., Wei, Y., Gao, B., Zhu, B., He, L., 2021. A Model Predictive Control Approach with Slip Ratio Estimation for Electric Motor Anti-Lock Braking of Battery Electric Vehicle. *IEEE Transactions on Industrial Electronics,* Volume 69(9), pp. 9225–9234

Kim, J., Lee, J., 2013. Real-Time Estimation of Maximum Friction and Optimal Slip Ratio Based on Material Identification for a Mobile Robot on Rough Terrain*. In:* 13th International Conference on Control, Automation and Systems (ICCAS 2013), pp. 1708–1713

Li, W., Du, H., Li, W., 2016. A New Torque Distribution Strategy for Blended Anti-Lock Braking Systems of Electric Vehicles Based On Road Conditions And Driver's Intentions. *SAE International Journal of Passenger Cars-Mechanical Systems,* Volume 9, pp. 107–115

Lin, C.M., Le, T.L., 2017. PSO-Self-Organizing Interval Type-2 Fuzzy Neural Network for Antilock Braking Systems. *International Journal of Fuzzy Systems*, Volume 19, pp. 1362–1374

Mirzaei, A., Moallem, M., Mirzaeian, B., Fahimi, B., 2005, September. Design of an Optimal Fuzzy Controller for Antilock Braking Systems. In *2005 IEEE Vehicle Power and Propulsion Conference*, pp. 823–828

Mirzaeinejad, H., 2018. Robust Predictive Control of Wheel Slip in Antilock Braking Systems Based On Radial Basis Function Neural Network. *Applied Soft Computing*, Volume 70, pp. 318–329

Nugraha, A.A., Sumarsono, D.A., Adhitya, M., Prasetya, S., 2021. Development of Brake Booster Design for Electric City Cars. *International Journal of Technology*. Volume 12(4), pp. 802–812

Oleksowicz, S.A., Burnham, K.J., Southgate, A., McCoy, C., Waite, G., Hardwick, G., Harrington, C., McMurran, R., 2013. Regenerative Braking Strategies, Vehicle Safety and Stability Control Systems: Critical Use-Case Proposals. *Vehicle System Dynamics*, Volume 51(5), pp. 684–699

Rajendran, S., Spurgeon, S., Tsampardoukas, G., Hampson, R., 2018. Intelligent Sliding Mode Scheme for Regenerative Braking Control. *IFAC-PapersOnLine*, Volume 51(25), pp. 334–339

Reif, K., 2014. *Brakes, Brake Control and Driver Assistance Systems*. Weisbaden, Germany, Springer Vieweg

Sergio, M.S., Mara, T., 2010. *Active Braking Control Systems Design for Vehicles.* London, UK: Springer.

Shah, D.A., Yu, L., Liu, X., Zheng, S., 2018. A New Design Of Main Cylinder Electric Booster For Brake-By-Wire System. *In:* International Design Engineering Technical Conferences and Computers and Information in Engineering Conference, Volume 2018, p. 85570

Tehrani, M.M., Hairi-Yazdi, R., Haghpanah-Jahromi, B., Esfahanian, V., Amiri, M., Jafari, R. 2011. Design of an Anti-Lock Regenerative Braking System for A Series Hybrid Electric Vehicle. *International Journal of Automotive Engineering*, Volume 1(2), pp. 16-20.

Topalov, A., Oniz, Y., Kayacan, E., Kaynak, O., 2011. Neuro-fuzzy Control of Antilock Braking System Using Sliding Mode Incremental Learning Algorithm. *Neurocomputing,* Volume 74(11), pp. 1883–1893

Tur, O., Ustun, O., Tuncay, R.N., 2007. An Introduction to Regenerative Braking of Electric Vehicles as ABS*. In:* IEEE Intelligent Vehicles Symposium, Volume 2017, pp. 944–948

Usman, M., Knapen, L., Vanrompay, Y., Bellemans, T., Janssens, D., Wets, G., 2016. A Coordinated Framework for Optimized Charging of EV Fleet in Smart Grid. *Procedia Computer Science*, Volume 94, pp. 332–339

Wang, W.Y., Chen, M.C., Su, S.F., 2012. Hierarchical T–S Fuzzy-Neural Control of Anti-Lock Braking System and Active Suspension in a Vehicle. *Automatica*, Volume 48(8), pp. 1698–1706

Yazicioglu, Y., Unlusoy, Y.S., 2008. A Fuzzy Logic Controlled Anti-Lock Braking System (ABS) For Improved Braking Performance and Directional Stability. *International Journal of Vehicle Design*, Volume 48(3-4), pp. 299–315

Yuan, L., Chen, H., Ren, B., Zhao, H., 2015. Model Predictive Slip Control for Electric Vehicle With Four In-Wheel Motors. *In:* 34th Chinese Control Conference (CCC), Volume 2015, pp. 7895-7900

Yusivar, F., Haslim, H.S., Farabi, Y., Nuryadi, K., 2015. New Control Scheme for Combined Regenerative and Mechanical Brakes in Electric Vehicles. *International Journal of Technology*, Volume 6(1), pp. 44–52

Yu, L., Liu, X., Liu, X., 2016. Analysis of Energy Consumption on Typical Main Cylinder Booster Based Brake-by-Wire System (No. 2016-01-1955). *SAE Technical Paper*, Volume 2016

Zhang, J.L., Yin, C.L., Zhang, J.W., 2010. Improvement Of Drivability and Fuel Economy with A Hybrid Antiskid Braking System In Hybrid Electric Vehicles. *International Journal of Automotive Technology*, Volume 11(2), pp. 205–213